that accounts for the variation of $\overline{u^2}$ in the streamwise direction for the corresponding product. However, these two models are notably limited in comparison with the Hanjalic-Launder model, which accounts for variations of the shear stress in both directions in addition to the $\overline{u^2}$ variations. It should, however, be noted that all the models would produce similar results in an isotropic turbulence flowfield.

The model of Cormack et al. was evaluated only for $\overline{vvv}$ and $\overline{uvv}$ since the values computed for $\overline{uuv}$ using its original form were not high enough to estimate the factor C_p within a reasonable range (see Fig. 2). Otherwise, the values of C_p derived using the model of Cormack et al. were the lowest, indicating that this model gives the best agreement with experiments when used in its original form.

Conclusions

1) The triple-velocity products need to be predicted accurately in the reattaching shear layer in order to evaluate appropriately the diffusion process of the Reynolds stress. The behavior of the triple-velocity products in such a complex turbulent flow is different from that in simpler flows.

2) All the existing algebraic models for the triple-velocity products underpredict the levels of $\overline{u_i u_j u_k}$ in the reattaching shear layer. The predicted levels can easily be improved by using a correction factor.

3) With the exception of the model of Hanjalic-Launder, all models cannot be improved simply by employing a single value for C_p. Thus, it is difficult to obtain a unique value for the correction factor. This is because the Hanjalic-Launder model is the only one that includes the generation terms due to Reynolds stresses.

Finally, it was observed that none of the above models accurately predict the overall levels of the triple-velocity products, primarily because the convection effect of the triple-velocity products is never considered at all. This effect may be small in simple shear layers but is significantly large when the shear layer reattaches on a solid wall, creating high turbulence energy near the wall and, subsequently, these high levels are transported in the downstream direction. In consequence, a transport model for $\overline{u_i u_j u_k}$ that takes this process into account must be developed and tested for complex turbulent flows.

Acknowledgment

This work was sponsored by NASA Lewis Research Center under Grant NAG 3-546 monitored by Mr. Thomas VanOberbeke.

References

[1]Chandrsuda, C. and Bradshaw, P., "Turbulence Structure of a Reattaching Mixing Layer," *Journal of Fluid Mechanics*, Vol. 110, 1980, pp. 171-194.

[2]Daly, B. J. and Harlow, F. H., "Transport Equations in Turbulence," *Physics of Fluids*, Vol. 13, No. 11, 1970, pp. 2634-2649.

[3]Hanjalic, K. and Launder, B. E., "A Reynolds Stress Model of Turbulence and Its Application to Thin Shear Flows," *Journal of Fluid Mechanics*, Vol. 52, Pt. 4, 1972, pp. 609-638.

[4]Shir, C.C., "A Preliminary Numerical Study of Atmospheric Turbulent Flows in the Idealized Planetary Boundary Layer," *Journal of Atmospheric Science*, Vol. 30, Oct. 1973, pp. 1327-1339.

[5]Cormack, D. E., Leal, L. G., and Seinfeld, J. H., "An Evaluation of Mean Reynolds Stress Turbulence Models: The Triple-Velocity Correlation," *ASME Journal of Fluids Engineering*, Vol. 100, March 1978, pp. 47-54.

[6]Amano, R. S. and Goel, P., "Computations of Turbulent Flow Beyond Backward-Facing Steps by Using Reynolds-Stress Closure," *AIAA Journal*, Vol. 23, Sept. 1985, pp. 1356-1361.

Numerical Evaluation of Propeller Noise Including Nonlinear Effects

K. D. Korkan* and E. von Lavante†
Texas A&M University, College Station, Texas
and
L. J. Bober‡
NASA Lewis Research Center, Cleveland, Ohio

Introduction

THE continued pressure on aircraft manufacturers by communities and regulatory agencies to reduce noise levels requires a thorough analysis of the characteristics of the acoustic field induced by the propulsion unit. To this end, the accurate determination of noise levels generated specifically by propellers has been the subject of numerous experimental and theoretical studies. Recent studies have utilized the Ffowcs Williams-Hawkings formulation,[1] an extension of Lighthill's theory,[2,3] to make significant contributions to the theory and numerical computation of helicopter rotor and propeller noise.[4] However, the linear character of the present acoustic calculations still does not account for the quadrupole noise term, but does give reasonable correspondence with experiment up to transonic tip speeds. In the present study, the propeller noise in the acoustic near field is determined by integration of the pressure-time history in the tangential direction of a numerically generated flowfield about the SR-3 propfan, including the shock wave system in the vicinity of the propeller tip. As a result, the quadrupole source terms are accounted for in the present acoustic analysis, which yields overall sound pressure levels and the associated frequency spectra as a function of observer location.

Prediction of the Transonic Flowfield

The propfan configuration used in this analysis is an eight-blade SR-3 series propeller with a radius of 12.25 in. and blade angle at three-quarter radius of 61.3 deg. The analysis was applied to this configuration operating at several different freestream Mach numbers. The helical tip Mach numbers, advance ratios, rotational velocities, and power coefficients are shown in Table 1.

The transonic flowfield around the SR-3 propeller and axisymmetric spinner/nacelle configuration was computed using the NASPROP-E computer code developed by Bober et al.[5] The governing three-dimensional Euler equations are formulated in weak conservation law form, subject to transformation into body-fitted general coordinates. These equations correctly describe most of the physical phenomena, including nonlinear effects such as the propeller tip shock wave system. The equations were solved in the blade-to-blade physical domain using an implicit finite difference approximate factorization scheme. Since central differencing was applied, it was necessary to add numerical damping to assure stable time marching. It is assumed that the periodicity of the flow limits the size of the computational domain to the region between two adjacent blades. Typically, the solution method used 45 points in the axial direction, 21 points in the radial direction, and 11 points in the circumferential

Received April 22, 1985; revision received Aug. 12, 1985.

*Associate Professor, Aerospace Engineering Department, Associate Fellow AIAA.
†Assistant Professor, Aerospace Engineering Department. Member AIAA.
‡Head, Propeller Aerodynamics Section. Member AIAA.

direction. A segment of the grid in the axial-radial plane is shown in Fig. 1. The program provides results in terms of density ρ, pressure P, axial, tangential, and radial velocities, and total specific energy at each node point in the computational grid.

Near-Field Noise Evaluation

The overall sound pressure level (OASPL) within the near field was calculated in the present analysis by noting that a stationary observer at any point in the flowfield would experience pressure fluctuations with respect to time as each point along a coordinate line in the circumferential direction from blade to blade passed through the observer location.

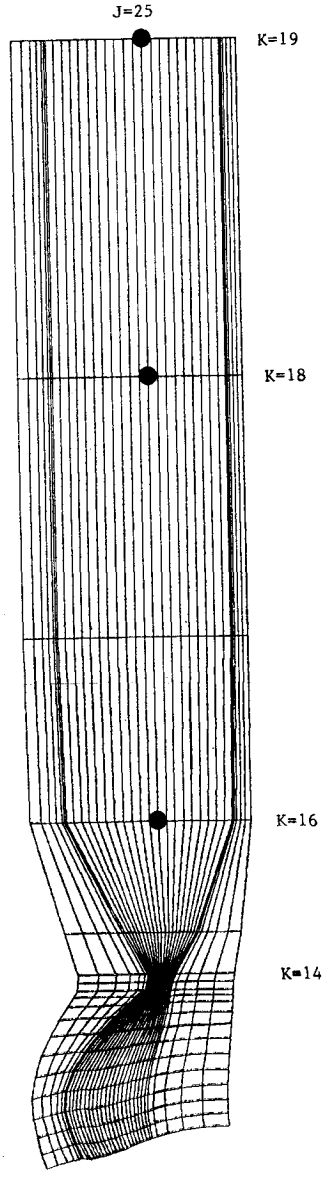

Fig. 1 Near-field grid in radial-axial plane.

Table 1 Operating conditions[a]

Case no.	rpm	M_∞	M_{hel}	C_p
1	5,443	0.50	0.71	1.96
2	6,573	0.60	0.86	1.91
3	7,072	0.65	0.93	1.91
4	7,550	0.70	1.00	1.89
5	8,039	0.75	1.08	1.79
6	8,495	0.80	1.14	1.71
7	8,933	0.85	1.21	1.53
8	9,500	0.90	1.29	—

[a]For all operating conditions, $J=3.06$, $\beta_{3/4}=61.3$ deg, $R=12.25$ in.

The transformation to the time domain was made using the relation, $\Delta t=\phi/\omega$, where ω is the rotational speed in radians/second, ϕ the circumferential angle in radians between two points, and Δt the time interval between passage of the two points located between the propeller blades. The calculation of OASPL now involves the pressure distribution between two periodic boundary surfaces, which correspond to a time period, $\Delta T=2\Pi/N\omega$, where N is the number of blades. The OASPL at a point in the flowfield can then be determined from the expression,

$$\text{OASPL}=10\log_{10}\left[\frac{P^2_{\text{rms}}}{P^2_{\text{ref}}}\right] \tag{1}$$

where $P_{\text{ref}}=20\mu\text{Pa}$ and

$$P^2_{\text{rms}}=\frac{1}{(T_2-T_1)}\int_{T_1}^{T_2}P^2(t)\,dt \tag{2}$$

with $(T_2-T_1)\gg\Delta T$. This analysis can be carried out at each point in the axial-radial plane once the total flowfield has been specified and can provide a OASPL map for the entire physical domain of the flowfield.

Specific information about the SPL at harmonics of the blade passing frequency was obtained by means of a Fourier analysis. The pressure-time history was represented by a Fourier series, where the acoustic pressure P can be expressed as $P_i-a_0/2$, where a_0 is the first Fourier coefficent. When the integral equation for P^2_{rms} is evaluated, the cross-product terms in the Fourier series vanish and Eq. (2) is written as

$$P^2_{\text{rms}}=\tfrac{1}{2}\sum_{k=1}^{\infty}(a_k^2+b_k^2) \tag{3}$$

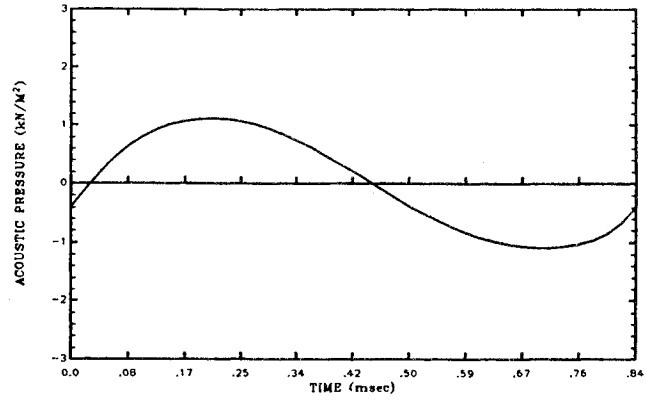

(A) ACOUSTIC PRESSURE TIME-HISTORY

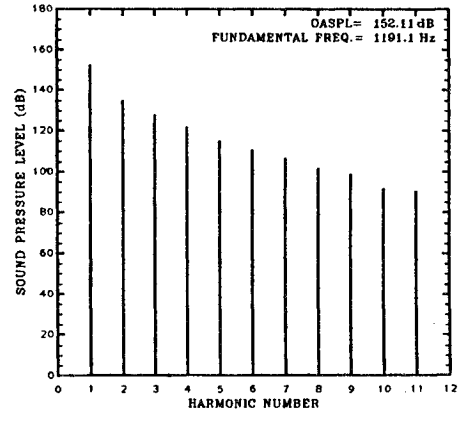

(B) SPECTRAL CONTENT OF NOISE SIGNATURE

Fig. 2 Calculated pressure-time history and spectral content at $2.703R_{\text{tip}}$ for helical tip Mach number of 1.21.

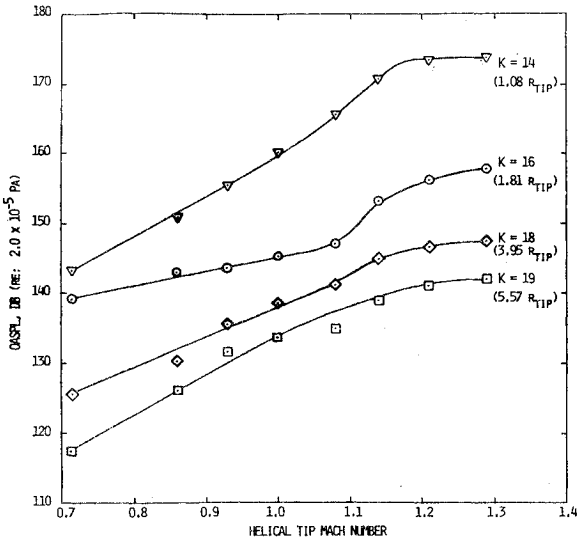

Fig. 3 Variation of OASPL with helical tip Mach number at $J=25$ (disk plane) at four radial locations.

Table 2 Comparison of predicted SPL levels with experimental data from Dittmar et al.[6,7]

Helical tip Mach number	Position 2[a]		Postion 5[b]	
	Experiment	Prediction	Experiment	Prediction
0.863	129.4	130	133.8	136.4
1.00	140.7	138.5	141.2	141.9
1.07	141.8	141	143.9	143.9
1.14	138.7	144	143.2	148.1
1.21	139.4	145	143.5	149.8

[a] $r=3.93R_{tip}$. [b] $r=2.95R_{tip}$.

and the SPL of the kth harmonic of the blade passing frequency is expressed as

$$\mathrm{SPL}_k = 10 \log_{10}[(a_k^2 + b_k^2)/(\sqrt{2}P_{ref})]^2 \quad (4)$$

Results and Discussion

The analysis procedure outlined above was applied to the eight cases shown in Table 1 for four points in the near field as indicated in Fig. 1. It may be noted that all of the points are located in the high-resolution area of the computational grid system, since the relatively coarse grid outside of this region yielded highly unreliable results in terms of OASPL. Likewise, the OASPL results at points located far from the propeller blade were not acceptable due to the relatively large influence of the numerical damping and boundary conditions.

Applying this method to the radial location of $1.82R_{tip}$ for a helical tip Mach number of 1.21, the calculated acoustic pressure-time history and spectral content is shown in Fig. 2. As noted, the acoustic time history is well behaved and the spectral content shows the proper decrease as the harmonic number increases. The OASPL, as calculated by this method, is shown in Fig. 3 as a function of helical tip Mach number and radial location at a fixed axial position in the propeller disk plane. As noted in Table 2, the theoretical predicted OASPL values compare well with the experimental noise quantities of Dittmar et al.[6,7] up to a helical tip Mach number of 1.07 at two microphone locations in the acoustic field of the propeller disk plane. It is postulated that very close to the propeller blade tip ($K=14$, $r=1.08R_{tip}$), the OASPL values first show a linear increase with helical tip Mach number, followed by a constant OASPL value. The influence of the shock wave system in the vicinity of the blade tip ($K=16$, 18; $r=1.81$, $3.95R_{tip}$) then becomes more pronounced, resulting in a sharp increase of the OASPL at a helical tip Mach number of approximately 1.1. As the point of calculation moves farther away from the blade tip, the influence of the shock wave system decreases where at $r=5.57R_{tip}$ ($K=19$), the OASPL curve shows the typical linear dependence on helical tip Mach number followed by a constant OASPL value.

Conclusions

The acoustic calculation method in this Note has been shown to be useful in the determination of acoustic near-field sound pressure level and frequency spectra for a range of operating conditions of the SR-3 propfan, yielding values that are comparable to experiment. Several areas have been suggested in which further study is needed and are currently under investigation. These include the effect of numerical damping, dependence of the acoustic values on the computational grid, and determination of the far-field acoustic characteristics.

Acknowledgment

This work was supported by NASA Lewis Research Center Grant NAG 3-354.

References

[1]Ffowcs Williams, J. E. and Hawkings, D. L., "Sound Generated by Turbulence and Surfaces in Arbitrary Motion," *Philosophical Transactions of the Royal Society of London*, Vol. A264, 1969.

[2]Lighthill, M. J., "On Sound Generation Aerodynamically: I. General Theory," *Proceeding of the Royal Society of London*, Vol. A221, 1952.

[3]Lighthill, M. J., "On Sound Generation Aerodynamically: II. Turbulence as a Source of Sound," *Proceedings of the Royal Society of London*, Vol. A222, 1954.

[4]Farassat, F., "Linear Acoustic Formulas for Calculation of Rotating Blade Noise," *AIAA Journal*, Vol. 19, Sept. 1981, pp. 1122-1130.

[5]Bober, L. J., Chaussee, D. S., and Kutler, P., "Prediction of High Speed Propeller Flow Fields Using a Three-Dimensional Euler Analysis," NASA TM 83065, 1983 (also AIAA Paper 83-0188).

[6]Dittmar, J. H., Jeracki, R. J., and Blaha, B. J., "Tone Noise of Three Supersonic Helical Tip Speed Propellers in a Wind Tunnel," NASA TM 79167, 1979.

[7]Dittmar, J. H. and Jeracki, R. J., "Additional Noise Data on the SR-3 Propeller," NASA TM 81736, 1981.

Constraints of the Structural Modal Synthesis

Jon-Shen Fuh* and Shyi-Yaung Chen*
Kaman Aerospace Corporation
Bloomfield, Connecticut

Structural Modal Synthesis

THE modal synthesis method has been a most active topic in structural dynamics since publication of Hurty's original paper.[1] In this method, a complex structure is treated as an assemblage of components, and modes of the structure are approximated by synthesizing component modes. To ensure that the components will act as a single structure, the geometric compatibility and/or force equilibrium conditions are imposed on the component inter-

Received Aug. 21, 1985; revision received Nov. 20, 1985.

*Senior Research Engineer. Member AIAA.